Published in final edited form as:
Brain Res Bull. 2012 January 4; 87(1): 21–29. doi:10.1016/j.brainresbull.2011.10.011.

Acute neuregulin-1 signaling influences AMPA receptor mediated responses in cultured cerebellar granule neurons

Catherine Fenster[a,b], **Detlef Vullhorst**[b], and **Andres Buonanno**[b]

Catherine Fenster: cfenste1@ashland.edu; Detlef Vullhorst: vullhord@mail.nih.gov; Andres Buonanno: buonanno@mail.nih.gov

[a]Department of Biology/Toxicology, 401 College Avenue, Ashland University, Ashland, OH 44805

[b]Section of Developmental Neurobiology, NICHD, Porter Neuroscience Research Center, Building 35, Room 2C-1002, 35 Convent Drive, Bethesda, MD 20892. 35 Convent Dr Room 2C1000, MSC 3713 Bethesda Md 20892-3713

[b]Section of Developmental Neurobiology, NICHD, Porter Neuroscience Research Center, Building 35, Room 2C-1000, 35 Convent Drive, Bethesda, MD 20892

Abstract

Neuregulin-1 (NRG1) is a trophic and differentiation factor that signals through ErbB receptor tyrosine kinases to regulate nervous system development. Previous studies have demonstrated that NRG1 affects plasticity at glutamatergic synapses in principal glutamatergic neurons of the hippocampus and frontal cortex; however, immunohistochemical and genetic analyses strongly suggest these effects are indirect and mediated via ErbB4 receptors on GABAergic interneurons. Here, we used cultured cerebellar granule cells (CGCs) that express ErbB4 to analyze the cell-autonomous effects of NRG1 stimulation on glutamatergic function. These cultures have the advantage that they are relatively homogenous and consist primarily of granule neurons that express ErbB4. We show that acute NRG1 treatment does not affect whole-cell AMPA or NMDA receptor (NMDAR) mediated currents in CGCs at 10–12 days *in vitro.* NRG1 also does not affect the frequency or amplitude of spontaneous AMPAR or NMDAR mediated miniature excitatory post-synaptic currents (mEPSCs). To further investigate the effects of NRG1 on activity-dependent plasticity of glutamatergic synapses in CGCs, we characterized the effects of activation of synaptic NMDAR with high-glyine/0 Mg^{2+} on AMPAR-mEPSC frequency and amplitude. We show that high-glycine induces a form of chemical long-term potentiation (chemLTP) in CGCs characterized by an increase in AMPAR-mEPSC frequency but not amplitude. Moreover, NRG1 induces a decrease in AMPAR-mEPSC frequency following chemLTP, but does not affect AMPAR-mEPSC amplitude. CGCs in our cultures conditions express low levels of GluR1, in contrast to dissociated hippocampal cultures, but do express the long isoform of GluR4. This study provides first evidence that (1) high-glycine can induce plasticity at glutamatergic synapses in CGCs, and (2) that acute NRG1/ErbB-signaling can regulate glutamatergic plasticity in CGCs. Taken together with previous reports, our results suggest that, similar to Schaeffer collateral to CA1 synapses, NRG1 effects are activity dependent and mediated via modulation of synaptic AMPARs.

Keywords

cerebellar granule neurons; neuregulin-1; ErbB; chemical LTP; synaptic plasticity

Corresponding author: Catherine P Fenster, Department of Biology/Toxicology, 401 College Avenue, Ashland University, Ashland, OH 44805, office: (330) 231-8334, fax: (419)-289-5283, cfenste1@ashland.edu.

1. INTRODUCTION

Neuregulin-1 (NRG1) is a trophic and differentiation factor that signals through ErbB receptor tyrosine kinases to regulate nervous system development and function (reviewed in Adlkofer and Lai, 2000; Buonanno and Fischbach, 2001; Fischbach and Rosen, 1997). In the developed nervous system, neuregulin signals through ErbB4 to influence transmission and plasticity at glutamatergic synapses (Chen et al., 2010; Iyengar and Mott, 2008; Kwon et al., 2005; Pitcher et al., 2008). Specifically, acute activation of NRG1/ErbB4-signaling pathways inhibits both the induction and maintenance of LTP at CA3→CA1 synapses (Iyengar and Mott, 2008; Kwon et al., 2005; Pitcher et al., 2008). Given the well-established requirement of CA3→CA1 LTP in hippocampal-dependent learning (reviewed in(Siegelbaum and Kandel, 1991), understanding the mechanisms through which NRG1 regulates plasticity at these synapses has important implications. ErbB4 is abundantly expressed in GABAergic interneurons but expression is undetectable in principal glutamatergic neurons of the hippocampus and frontal cortex (Fazzari et al., 2010; Neddens and Buonanno, 2010; Neddens et al., 2011; Vullhorst et al., 2009); moreover, ablation of the ErbB4 gene in GABAergic interneurons, but not pyramidal neurons, blocks the inhibition of LTP induction by NRG1 (Chen et al., 2010). Therefore, NRG1-dependent effects on LTP are indirect in that they do not require ErbB4 signaling in CA1 pyramidal cells. Several lines of evidence support the idea that NRG1/ErbB4-signaling directly regulates postsynaptic function of glutamatergic synapses on ErbB4-expressing neurons. First, ErbB4 colocalizes with postsynaptic AMPA and NMDARs (Garcia et al., 2000; Ma et al., 2003; Ozaki et al., 1997) and the carboxyl-terminal PDZ-ligand domain of ErbB4 interacts directly with members of the family of MAGUK-type synaptic scaffolding proteins including PSD-95/SAP-90 (Garcia et al., 2000; Huang et al., 2000), indicating that ErbB4 receptors are positioned to directly modulate AMPA and NMDARs and/or associated regulatory proteins. Second, deletion of ErbB4 in PV-positive interneurons inhibits formation of functional glutamatergic synapses on these neurons (Ting et al., 2011), demonstrating that ErbB4 controls glutamatergic synapse development. Although central to understanding NRG1-dependent regulation of glutamatergic function and plasticity, the direct and acute effects of NRG1/ErbB4-signaling on the function of glutamatergic synapses and/or glutamate receptors in ErbB4-expressing neurons have been difficult to establish in hippocampal and/or cortical preparations.

In this study, we used cultured cerebellar granule cells (CGC) to test the hypothesis that acute NRG1-signaling influences NMDAR and AMPAR-mediated responses in ErbB4-expressing neurons. In the context of the current study, CGCs provide the following experimental advantages: (1) CGCs express ErbB4 and are capable of responding to NRG-1: For example, chronic NRG-1/ErbB4-signaling effects have been characterized, and include enhanced neurite outgrowth and enhanced expression of NR2C and $GABA_A$ β2 subunits, as well as activation of PI_3-kinase and cdk5 (Murphy and Bielby-Clarke, 2008; Rieff et al., 1999; Rieff and Corfas, 2006; Xie et al., 2004; Xie et al., 2007); (2) CGCs are well-characterized with regard to developmental and subcellular expression of AMPAR and NMDAR subtypes (Cull-Candy et al., 1998; Farrant et al., 1994; Fu et al., 2005), (3) CGCs are relatively homogenous, consisting of >95% granule neurons which form glutamatergic connections in culture, and (4) CGCs are small with few dendrites, allowing for high resolution recordings of AMPAR and NMDAR medicated responses using whole-cell voltage-clamp techniques (Fu et al., 2005; Lu et al., 2006; Silver et al., 1992).

To determine whether acute ErbB4 stimulation affects glutamatergic transmission in CGCs, we first characterized the effects of NRG-1β on AMPA and NMDAR-mediated whole-cell responses and mEPSCs in CGCs using whole-cell voltage clamp techniques. Because NRG1 effects may be activity-dependent, we also investigated the acute effects of NRG-1β and

ErbB-inhibition on AMPAR-mediated responses following chemical LTP induction via high-glycine/0 Mg^{2+}.

2. EXPERIMENTAL PROCEDURES

2.1 CGC cultures

CGCs were prepared as previously described (Losi et al., 2002) with minor modifications. Cerebella were harvested from 4–5 day old C57BL/6J mice. All procedures were approved by the IACUC at the NIH. Following induction of hypothermia, the cerebella from 2–3 mice were placed in cold Solution I (HBSS minus Ca^{++}, Mg^{++}, HCO_3^- and supplemented with 0.3% BSA and 14 mM glucose, 15 mM HEPES, 4.2 mM $NaHCO_3$, and 1.5 mM $MgSO_4 \cdot H_2O$). After removing meninges, cerebella were incubated in Solution I containing 0.05 % trypsin (Sigma, St. Louis, MO) for 5 min at 37°C. The solution was replaced with cold Stop Solution (Solution I containing 0.25% soybean trypsin inhibitor [Cat. No. 65035, Calbiochem, LaJolla, CA), and 0.04% DNAse I)]. Neurons were dissociated in Solution I by trituration on ice. Cells were pelleted and resuspended in CGC media [basal Eagle's medium supplemented with 10 % bovine calf serum, 2 mM glutamine (all from Invitrogen, Carlsbad, CA), Primocin (Amaxa BioSystems, Gaithersburg, MD) and 25 mM KCl] and maintained at 37°C, 5% CO_2. Neurons were plated in 24 well dishes at density of 1×10^6 cell/ml directly onto acid-washed coverslips coated with 50 μg/ml poly-D lysine. After five days *in vitro*, the medium was changed to low (5 mM) KCl to enhance functional synapse formation [minimal essential medium with 5 mg/ml glucose (Invitrogen) supplemented with 10 μM cytosine-arabanofuanoside (Sigma), 2 mM glutamine, insulin transferrin supplement (Sigma), and Primocin (Amaxa BioSystems).

2.2 Western blot analysis

Hippocampal cultures and CGC cultures were rinsed with cold PBS and lysed in buffer (50mM EDTA, 150mM NaCl, 50mM Tris pH 7.4, 1% Triton X-100) containing Complete Protease Inhibitor Cocktail (Roche, Indianapolis, IN). Lysates were cleared by centrifugation at 12,000 RPM for 5 min at 4° C using a 5415C microcentrifuge (Eppendorf, Hamburg, Germany). Proteins were quantified using the BioRad Protein Assay Reagent (BioRad, Hercules, CA). Proteins (20 μg/lane) were electrophoretically separated using Novex Tris-Glycine 4–12% gradient gels and electroblotted onto nitrocellulose membranes. Immunoblots were blocked (5% nonfat milk in 0.1% Tween-20 in TBS) and separately probed with the following primary antibodies: rabbit polyclonal against the C-terminus of the long isoform of GluR4 (1:1000, Cat No. 06-308, Millipore, Billerica, MA); rabbit polyclonal anti-GluR1 (1:1000, Cat No. AB1504, Millipore); rabbit monoclonal anti-ErbB4 mAB-10 (1 μg/ml; (Vullhorst et al., 2009); polyclonal anti-NR2B (1:1000, Cat No. 06-600, Millipore), and rabbit polyclonal anti-NRG1 (1:500, Cat No. 348, Santa Cruz Biotechnology, Santa Cruz, CA), mouse monoclonal anti-clathrin heavy chain (1:2000, clone TD.1, Cat No. sc-12734, Santa Cruz). Blots were extensively washed in TBS-T and then incubated with either donkey-anti-rabbit or sheep-anti-mouse IgG conjugated to HRP. Signals were visualized with the ECL Plus Western Blotting Detection system (GE Healthcare, Piscataway, NJ). As an additional loading control, blots were stripped and re-probed with antibodies for GAPDH (0.5 μg/ml, Millipore), α– tubulin (Cell Signaling Technology, Beverly, MA) or clathrin heavy chain (1:2000, Cat No. 12734, Santa Cruz).

2.3 Electrophysiology

All recordings were performed at room temperature from CGCs at 9–12 days *in vitro.* Electrodes were made from thin-wall borosilicate glass capillaries (Wiretrol II; Drummond) with a two-stage vertical puller. Recording electrodes were filled with intracellular solution containing (in mM): 0.6 EDTA, 5 ATP Mg Cl_2, 0.2 GTP, 145 potassium gluconate, 10

HEPES, pH 7.2 with KOH and adjusted to300 mOsM with sucrose. Typical pipette resistances were 3–5 MΩs. Whole-cell voltage-clamp recordings were performed using an Axopatch 200B capacitor-feedback patch clamp amplifier (Axon CNS Molecular Devices, Sunnyvale, CA) at a holding potential of −60 mV. Currents were filtered at 1 kHz and digitized at 10 kHz using a Dell computer equipped with Digidata 1322 analogue-to-digital board and pClamp10 software (Axon CNS Molecular Devices). Access resistance was monitored throughout the recording using transient current responses to hyperpolarizing 5 mV pulses. Off-line data analysis and fitting were performed with Clampfit10.2 (Axon CNS Molecular Devices). CGCs with capacitance >10 pF (unlikely to represent CGCs) or exhibiting a change in access resistance >10 % were excluded from the analysis.

NMDAR and AMPAR-mEPSCs were identified from continuous recordings using Clampfit 10 (Axon CNS Molecular Devices) and the software's event detection template matching functions. If AMPAR-mEPSC frequencies were < 0.04 Hz at baseline recordings were terminated and/or omitted from the analysis. NMDAR-mEPSC and AMPAR-mEPSC decays were fit using Clampfit 10 (Axon CNS Molecular Devices) from averages of 1–20 consecutive events selected using the software's event detection template matching functions. Current decays were fit using a single-exponential equation [$I(t) = I \times \exp(-t/\tau)$].

2.4 Recording Solutions

Glass cover slips with CGCs or hippocampal neurons were placed in a recording chamber (total volume ~0.5 ml) with a solution exchange rate of 5 ml/min. Control bath extracellular solution (ECF) contained (in mM) 145 NaCl, 5 KCl, 1 $MgCl_2$, 1 $CaCl_2$, 5 HEPES, 5 glucose, as well as 10 μM D-serine and 500 nM TTX (all from Sigma) and adjusted to 325 mOsM with sucrose and pH 7.4. Recording solutions used to isolate AMPAR and NMDAR-mediated whole-cell currents and mEPSCs were delivered using a gravity-fed Y-tubing system as described (Murase et al., 1989). The outflow of the Y-tubing system was placed approximately 50 microns from the recorded cell. Throughout the experiment, cells were continually perfused through the Y-tubing system with either control ECF or specified recording ECF. For recording of whole-cell NMDAR-currents, NMDA (200 μM, Tocris, Ellisville, MO) was applied in Mg^{2+}-free ECF also containing 500 nM TTX (Calbiochem), 50 μM bicuculline (to block $GABA_A$ receptors, from Tocris). NMDAR- mediated mEPSCs were recorded in Mg^{2+}-free ECF also containing 500 nM TTX, 50 μM bicuculline, 20 μM D-serine, and 5 μM NBQX (to block AMPARs) as described (Prybylowski et al., 2002). To record whole-cell AMPAR-mediated currents, kainate (KA) was applied in ECF also containing 1 mM $MgCl_2$, 500 nM TTX, 50 μM bicuculline. To verify that kainate-evoked responses were mediated by AMPARs, in a subset of cells, GYKI 52466 (50 μM), an AMPAR specific receptor antagonist at this concentration, was applied prior to and during kainate application. AMPAR-mediated mEPSCs were recorded in ECF containing 1 mM $MgCl_2$, 500 nM TTX, 50 μM bicuculline (as described (Losi et al., 2002). For treatment with high-glycine/0 Mg^{2+}, cells were exposed to high-glycine solution (ECF containing 200 μM glycine, 0 $MgCl_2$, 2 mM $CaCl_2$, 0.1 μM strychnine) for 5 minutes at room temperature. NRG-1β (recombinant EGF-like domain, corresponding to NRG1-β1, amino acids 176–246, from R&D Systems, Minneapolis, MN) was used at a concentration of 2 nM (from stocks of 5 μM in PBS with 0.1% BSA) and was added to the recording solution applied through the Y-tubing system. Vehicle control corresponded to an equal volume of vehicle (0.1% BSA in PBS). PD158780, a pan-ErbB receptor antagonist, was used at a concentration of 10 μM (Calbiochem).

2.5 Statistical Analyses

Homogeneities of variances were verified (Levene Statistic) and one-way ANOVAs with Tukey HSD post-hoc comparisons ($\alpha = 0.05$) were used to evaluate differences between

treatment groups (SPSS 12.1, SPSS Chicago, IL). In some cases, independent sample *t*-tests (two-tailed) were used to evaluate differences between treatment groups. To test the null hypothesis that high-glycine/0 Mg^{2+} affected the distribution of amplitudes, an independent-samples Kolmogorov-Smirnov test was used to compare amplitudes prior to and following high-glycine treatment (25 events randomly selected occurring prior to and between 5 and 8 minutes following treatment onset, n = 10 cells). To assess differences between groups in response to treatment across time, we used repeated-measures ANOVAs. Data are presented as mean ± standard deviation (SD) and as standard error (SEM) in cases where data for an individual sample represents the mean of several events.

3. RESULTS

3.1 Expression of ErbB4 and GluR4 (GluR4 long) in dissociated CGCs

In our electrophysiological assays, we used CGCs > 9 days *in vitro* because AMPA and NMDAR-mediated mEPSCs were rarely observed in younger cultures (see also (Losi et al., 2002). By Western blot analysis, GluR1 was undetectable in CGCs between DIV 5–10 while GluR4 was readily observed at DIV 5, steadily increasing through DIV 10 (Fig. 1A). Conversely, GluR1 protein levels were high in DIV 16 hippocampal neurons while GluR4 was very low. ErbB4 was detected at all time points, with comparable protein levels in DIV 5 CGCs and hippocampal cultures, but diminishing somewhat after that (Fig. 1B). Of note, ErbB4 was detected by immunocytochemistry in both excitatory and inhibitory neurons in our cultures (data not shown). NRG1 expression was strong at DIV 5 but undetectable afterwards, suggestive of a lack of survival of NRG1-expressing cells under our culture conditions (Fig. 1C). Our data indicate that the long isoform of GluR4 is likely a predominant subunit of functional AMPARs in our cultures, consistent with *in vivo* expression pattern of AMPAR subunits in the cerebellum (e.g., Gallo et al., 1992). Moreover, the lack of endogenous NRG1 expression after DIV 5 was convenient as it facilitated the interpretation of responses to exogenously added NRG1 (see below).

3.2. Acute treatment of CGCs with NRG1 does not affect NMDAR or AMPAR-mediated whole-cell currents or mEPSCs

Whole-cell AMPAR currents were activated using kainate (KA, 50 μM). To verify these currents were mediated through AMPARs, whole-cell KA responses were recorded in the presence and absence of GYKI-52466 (50 μM), an AMPAR antagonist at this concentration. GYKI-52466 inhibited KA-activated currents confirming they are mediated through AMPARs (Fig. 2A). To assess the effects of NRG1 on whole-cell AMPAR currents, after obtaining at least two stable whole-cell KA responses, a recombinant protein encompassing the EGF-like domain of human NRG-1β (2 nM; hereafter referred to as NRG1) or vehicle control was added to the recording solution and whole-cell KA responses were recorded at 2 and 4 minutes following treatment onset (Fig. 2B). NRG1 did not affect whole-cell KA responses under these recording conditions. Specifically, changes in whole-cell AMPAR-current amplitude (calculated as the average of two peak KA current amplitudes obtained post-treatment minus baseline) were not different for NRG1 treated CGCs as compared with control ($t_{(24)} = 0.008$; $P = 0.9$) (Fig. 2C). Inspection of KA responses for individual cells further confirmed that NRG1 has no clear effect on KA currents (Fig. 2D).

Given evidence that ErbB4 receptors are enriched at postsynaptic densities (Garcia et al., 2000; Huang et al., 2000), acute NRG1/ErbB4-signaling may selectively affect the function of postsynaptic receptors. Therefore, we next tested whether of NRG1 modified the frequency or amplitude of AMPAR-mEPSCs, which are mediated by postsynaptic AMPARs in response to spontaneous presynaptic transmitter release (Fig. 3A). AMPAR-mEPSCs were recorded for several minutes prior to and following treatment with either NRG1 (2

nM), the pan ErbB kinase inhibitor PD158780 (10 μM), or vehicle control (Fig. 3B). PD158780 was used to assess the extent of endogenous ErbB-signaling and possible occlusion of NRG1 effects by endogenous ErbB-signaling. However, AMPAR-mEPSC amplitude and frequency were not affected by treatments with NRG1 or PD158780 relative to control (Fig. 3C and D). Specifically, no significant differences between treatment groups with time were observed for AMPAR-mEPSC amplitude ($F_{(2,23)} = 1.04$, $P = 0.35$; repeated measures ANOVA for time*treatment interaction); in addition, although significant differences between treatment groups with time were observed for AMPAR-mEPSC frequency ($F_{(2,23)} = 3.6$, $P = 0.04$; repeated measures ANOVA for time*treatment interaction), post-hoc comparisons indicate that neither treatment group was significantly different from control (Fig. 3D).

We next investigated effects of acute NRG1-signaling on NMDAR function by measuring whole-cell NMDA-activated currents and NMDAR-mEPSCs before and after perfusion with NRG1. To assess effects on whole-cell NMDA currents, after obtaining 1–2 stable peak whole-cell NMDA (200 μM) responses, NRG1 (2 nM), PD158780 (10 μM) or vehicle control were added to the perfusion solution and additional NMDA-responses were recorded following treatment onset (Fig. 4A). Whole-cell NMDAR-currents were not different after NRG1; specifically, the change (post-treatment minus baseline) in current amplitudes was not different between treatment groups ($F_{(2,22)} = 0.63$, $P = 0.54$; one-way ANOVA) (Fig. 4B). Mean ± SD currents prior to and following treatments were 364 ±145 pA and 362 ± 149 for control cells, 359 ± 126 and 345 ± 135 for NRG1 treated cells, and 290 ± 138 and 286 ± 140 for PD158780 treated cells. To address the possibility that NRG1 effects might be inhibited by dialysis with intracellular recording solution, in a separate experiment, we treated cells with NRG1 or vehicle control for 4 minutes immediately before breaking into the cell. Cells were maintained in respective treatments, voltage-clamped and then whole-cell NMDA currents were recorded within approximately 6 minutes of treatment onset. As before, NRG1 had no effect as peak and steady-state whole-cell NMDAR current amplitudes (pA/pF) did not differ between treatment groups (data not shown). Next, NMDAR-mEPSCs were recorded for several minutes prior to and following perfusion with NRG1 or vehicle control (Fig. 4C). Means for peak current amplitude, frequency and τ-decay were not different prior to or following 2–4 min treatment with NRG1 (Fig. 4D). In summary, the above results demonstrate that acute NRG1/ErbB4-activation in CGCs does not appreciably affect AMPAR or NMDAR-mediated currents under baseline conditions.

3.3 Treatment with high-glycine increases AMPAR-mediated mEPSCs frequency in CGCs

Our next goal was to investigate the possibility that acute NRG1 treatment influences glutamatergic transmission in CGCs in an activity-dependent manner, through a mechanism involving synaptic NMDAR activation. For primary hippocampal neurons, treatment with high-glycine/0 Mg^{2+} leads to activation of synaptic NMDARs (Lu et al., 2001) and, similar to LTP induced by electrical stimulation, induces an increase in synaptic GluR1 as well as increased AMPAR-mEPSC frequency and amplitude (Liao et al., 2001; Lu et al., 2001; Pickard et al., 2001). Moreover, following glycine-induced chemLTP, NRG1 induces internalization of GluR1 (Kwon et al., 2005). Although the mechanisms are unclear, these studies indicate that NRG1 may specifically affect dynamic trafficking of AMPARs in response to synaptic NMDAR activation.

We began by testing the effects of high-glycine/0 Mg^{2+} on AMPAR-mediated responses by continuously recording AMPA-mEPSCs for several minutes prior to, during and following treatment with control ECF or ECF with high-glycine/0 Mg^{2+} (Fig. 5A). Glycine-treated cells, relative to control, exhibited a significant increase in AMPAR-mEPSC frequency ($t_{(18)} = 2.5$, $P = 0.005$), whereas neither the mean amplitude ($t_{(18)} = 1.2$, $P = 0.18$; Fig. 5B) nor the distribution of amplitudes were affected by high-glycine ($P = 0.61$; independent-samples

Kolmogorov-Smirnov test). Glycine-treated cells exhibited an increase in AMPAR-mEPSC frequency of 86% ± 32% (mean ± SEM), whereas control cells exhibited only a 10% ± 10% increase. In a separate experiment, we assessed the effects of high-glycine on whole-cell AMPAR currents by comparing whole-cell KA current amplitudes prior to and following treatment onset with glycine or control. High-glycine did not affect whole-cell KA current amplitudes: KA current amplitudes prior to and following high-glycine were very similar (369 ± 198 pA prior and 370 ± 162 following glycine, n = 29 cells); by comparison, amplitudes prior to and following control were also very similar (235 ± 105 pA prior and 233 ±101 following control, n = 12 cells) (data not shown). Finally, we also assessed the effects of high-glycine/0 Mg^{2+} prior to going whole-cell (Fig. 5C). We repeated the experiment using this strategy because (i) intracellular dialysis with electrode solution could disrupt physiologically relevant intracellular pathways and cytoskeletal components, and (ii) our next goal was to assess NRG1 effects following high-glycine and CGCs which were to reseal after prolonged recording; thus, by initiating recording following high-glycine we were able to record the effects of NRG1 following chemLTP in a greater number of cells. Similar to results summarized above (Fig. 5A and 5B), cells treated with high-glycine/0 Mg^{2+} prior to going whole-cell (Fig. 5C) exhibited greater AMPAR-mEPSC frequencies relative to control ($t_{(40)} = 3.21$, $P = 0.002$), with no differences in AMPAR-mEPSC amplitude ($t_{(40)} = 1.11$, $P = 0.27$) (Fig. 5D). The observed increase in AMPAR-mEPSC frequency is consistent with the possibility that activation of synaptic NMDARs high-glycine/0 Mg^{2+} may facilitate the conversion of silent (i.e., AMPAR-lacking) into active (i.e., AMPAR-containing) synapses in CGCs, as suggested previously for hippocampal neurons (Liao et al., 2001).

3.4 Following high-glycine, NRG1 reduces AMPAR-mEPSC frequency

We next compared effects of NRG1, vehicle control and PD158780 on AMPAR-mEPSCs following chemLTP. In these experiments, cells were treated with 200 μM glycine and then immediately voltage-clamped. AMPAR-mEPSCs were then recorded for 4–6 min prior to treatment-onset with either PD158780, NRG1, or vehicle control (Fig. 6A). Normalized data are shown for better comparison for amplitude (Fig. 6B) and frequency (Fig. 6C) across time prior to and following treatment onset. Mean ± SD peak amplitudes at baseline (mean of data recorded between 1 and 3 minutes prior to treatment onset) and following treatments (mean of data recorded after 4 minutes of treatment onset) were 10.3 ± 1.5 pA and 9.6 ± 1.0 for PD15870 treated cells, 12.6 ± 5.3 and 15.0 ± 8.1 for control cells, and 17.0 ± 0.5 and 17.1 ± 9.0 for NRG1 treated cells. The average frequencies at baseline and following treatments were 0.19 ± 0.04 Hz and 0.33 ± 0.14 for PD15870, 0.17 ± 0.08 and 0.24 ± 0.12 for control cells, and 0.21 ± 0.07 and 0.11 ± 0.04 for NRG1-treated cells. Although treatments did not affect AMPAR-mEPSC amplitude ($F_{(2,22)} = 2.2$, $P = 0.14$; repeated measures ANOVA for time by treatment interaction) change in current amplitude), tthey did affect AMPAR-mEPSC frequency ($F_{(2,22)} = 13.42$, $P<0.001$) and post-hoc comparisons for change in frequency reveal a significant difference between NRG1 and control treatments ($P = 0.005$, post-hoc Tukey HSD). In summary, NRG1 reduces AMPAR-mEPSC frequency, but not amplitude, following high-glycine/0 Mg^{2+}in CGCs.

4. DISCUSSION

In the current study, we characterized the effects of NRG1 on NMDAR and AMPAR-mediated responses in dissociated CGCs cultures. CGCs are an especially attractive system for investigating NRG1/ErbB4-signaling effects because CGCs express ErbB4 and NRG1 have been shown to activate pathways downstream of ErbB4 in these cells (Murphy and Bielby-Clarke, 2008; Ozaki et al., 1997; Xie et al., 2004; Xie et al., 2007). In contrast, only a subset of cells express ErbB4 in cortical or hippocampal cultures or slice preparations

(Neddens and Buonanno, 2010; Vullhorst et al., 2009), which poses constraints on certain experimental approaches and interpretations.

The major unique findings of the current study are: (i) NRG1 has little effect on AMPAR or NMDAR-mediated currents in dissociated primary CGCs under baseline conditions (Fig. 2–4); (ii) Activation of synaptic NMDARs with high-glycine/0 Mg^{2+} potentiates AMPAR-mediated responses in dissociated CGCs. Specifically, high-glycine/ 0 Mg^{2+} enhances AMPAR-mEPSC frequency, but not does affect AMPAR-mEPSC or whole-cell AMPAR-mediated current amplitudes (Fig. 5); and (iii) Following treatment with high-glycine/0 Mg^{2+}, NRG1 induces a decrease in AMPAR-mEPSC frequency, but not amplitude (Fig. 6). In summary, our results suggest that acute NRG1 signaling may regulate glutamatergic plasticity in CGCs. Here we discuss the possibility that the NRG1 associated decrease in AMPAR-mEPSC frequency we observed only after chemLTP suggests NRG/ErbB-signaling effects are activity-dependent and may impinge selectively on recently mobilized AMPARs.

4.1 Expression of GluR4, GluR, NRG-1 and ErbB4 in CGCs

Although others have shown that CGCs exhibit a dramatic increase GluR1 mRNA and protein with increasing DIV when maintained in high K^+ (Longone et al., 1998), our results (Fig. 1) are consistent with previous studies demonstrating GluR1 expression does not increase in CGCs maintained low KCl (Condorelli et al., 1993; Mogensen and Jorgensen, 2000). Visual comparison of GluR1 and GluR4 immunoreactivity in hippocampal and CGC lysates suggests GluR4 is also expressed at high levels in CGCs relative to hippocampal neurons. Note that the GluR4 antibody used for the Western blot analysis recognizes the C-terminal tail of GluR4 (long cytoplasmic tail), but not GluR4C (short cytoplasmic tail). Overall ErbB4 expression was similar between CGCs and hippocampal lysates at DIV5 and decreased somewhat at later stages, consistent with previous studies (Rio et al., 1997). Importantly, while prominent at DIV5, NRG1 expression was undetectable after that, minimizing the possibility that endogenous NRG1 might confound effects of NRG-1 treatments in our experiments.

4.2 Acute NRG1/ErbB-signaling does not affect NMDAR or AMPAR function in CGCs under baseline conditions

Our results show NRG1 does not affect NMDAR or AMPAR currents in CGCs under baseline conditions in the presence of TTX. Although it is possible that the influence of NRG-1β was occluded by endogenous NRG-1-signaling, this explanation is unlikely considering that NRG-1 protein was undetectable after 5 days *in vitro* (Fig. 1), and because previous studies have shown that exogenously added NRG1 induces activation of ErbB4 in CGCs (e.g., (Murphy and Bielby-Clarke, 2008; Rieff and Corfas, 2006; Xie et al., 2007). Moreover, the ErbB tyrosine kinase inhibitor PD158780 did not affect NMDAR or AMPAR currents (Fig. 4 and 5), further suggesting that acute endogenous ErbB-signaling does not affect AMPAR or NMDAR function and/or spontaneous presynaptic vesicle release in CGCs under baseline conditions. The observation that NRG-1 does not affect basal glutamatergic synaptic transmission in CGCs is consistent with observations that glutamatergic transmission is not affected by NRG1/ErbB4 signaling in the hippocampus (Chen et al., 2010; Huang et al., 2000; Iyengar and Mott, 2008; Kwon et al., 2005; Pitcher et al., 2008).

4.3 Expression of chemical LTP induced by high-glycine/0 Mg^{2+} in CGCs

Although acute NRG1/ErbB4-signaling does not affect baseline glutamatergic transmission in the hippocampus, it does influence plasticity at glutamatergic synapses (Huang et al., 2000; Kwon et al., 2005; Iyengar and Mott, 2008, Pitcher et al., 2008), suggesting that acute

NRG1/ErbB4-signaling affects mechanisms underlying expression and maintenance of LTP. In cultured cortical and hippocampal neurons, high-glycine/0 Mg^{2+} induces “chemical LTP” that, similar to LTP evoked by electrical stimulation, is expressed as an increase in synaptic GluR1 and increases in AMPAR-mEPSC frequency (Liao et al., 2001) and/or amplitude (Liao et al., 2001; Lu et al., 2001). We were therefore prompted to investigate the effects of NRG1 on AMPR mediated responses following activation of synaptic NMDARs with high-glycine/0 Mg^{2+} in CGCs. Because chemLTP has not been reported in CGCs, we first needed to characterize the effects of high-glycine/0 Mg^{2+} on AMPAR-medicated responses in these cells.

For CGCs at 9–11 days *in vitro,* treatment with high-glycine/0 Mg^{2+} was associated with increased AMPAR-mEPSC frequency. The observed increase in AMPAR-mEPSC frequency could arise from either (i) mobilization of functional AMPARs to the synapse, resulting in an increase in the number of synapses with responses above detection threshold, and/or (ii) an increase in the probability of presynaptic vesicle release. Liao et al. (2001) demonstrated that in dissociated cortical neurons, either withdrawal treatment with high-glycine/0 Mg^{2+} induced an increase in AMPAR-mEPSC frequency (with no effect on amplitude) as well as a concomitant increase in mobilization of AMPAR subunits into morphologically silent synapses. The increase in AMPAR-mEPSC frequency, but not amplitude that we observed (Fig. 4 and 5) is therefore consistent with AMPAR recruitment to previously “silent” (i.e., AMPAR-lacking) synapses. Activation of AMPAR-lacking silent synapses in hippocampal pyramidal neurons involves trafficking of GluR1-containing receptors to the postsynaptic membrane (Liao et al., 2001; Shi et al., 1999). Subunit specific AMPAR trafficking is regulated largely by interactions between the unique C-terminal sequence of AMPAR subunits with PDZ-domain containing scaffolding proteins including PICK1, GRIP1, SAP97 and the TARPs (see review (Shepherd and Huganir, 2007). Consistent with previous studies (Gallo et al., 1992; Longone et al., 1998), GluR4 (GluR4L) is expressed in our CGC cultures (Fig. 1). Because GluR1 and GluR4 possess homologous C-terminal sequences, similar activity-dependent trafficking mechanisms may exist for these two subunits and may account for the increase in AMPAR-mEPSPs observed in cortical neurons (Liao et al., 2001) and CGCs (Fig. 4 and 5) with glycine-induced potentiation.

Although the most plausible explanations for the observed increase in AMPAR-mEPSCs (Fig. 5) involve activity-dependent regulation of AMPAR trafficking, we cannot exclude the possibility that high-glycine affects presynaptic vesicle release probability. LTP at synapses between mossy fibers and granule neurons parallel fibers in the cerebellum is NMDAR-dependent and involves changes in presynaptic excitability (D’Angelo et al., 1999; D’Angelo et al., 2005; Maffei et al., 2002); however, the relevance of these studies to CGC cultures is unclear. If the locus of potentiation is presynaptic, then we would expect to observe an increase in both AMPAR and NMDAR-mEPSC frequency; however, we found it difficult to reliably distinguish NMDAR-mEPSPs from background following high-glycine. Moreover, because NMDARs open spontaneously in 0 Mg^{2+} (Turecek et al., 1997) it would be difficult to distinguish NMDAR-mEPSPs from spontaneous opening of single NMDAR channels. In summary, although further studies are required to elucidate precise cellular mechanisms, our results demonstrate that high-glycine can induce plasticity at glutamatergic synapses in CGCs and are consistent activity-dependent trafficking of GluR4-containing AMPAR to previously silent synapses.

4.4 NRG1 affects glutamatergic plasticity in CGCs; what are the potential mechanisms?

In CGCs, NRG1 induces a decrease in AMPAR-mEPSC frequency when applied following activation of synaptic NMDARs with high-glycine/0 Mg^{2+}; however, whole-cell AMPAR-mediated currents and AMPAR-mEPSC amplitudes and amplitude distributions were unaffected (Fig. 6). Plausible explanations for decreased AMPAR-mEPSC frequency are

that NRG1 induces either (i) a reduction in synaptic AMPAR number or function, resulting in an increase in the number of synapses with responses below detection threshold, and/or (ii) a reduction in the probability of spontaneous presynaptic vesicle release. Given that NRG1 can induce internalization of GluR1 in hippocampal neurons in the early phases of LTP (Kwon et al., 2005), the decrease in AMPAR-mEPSC frequency observed in CGCs may similarly result from internalization of GluR1 and/or GluR4-containing AMPARs, as opposed to changes in presynpatic vesicle release. An alternate explanation for the NRG1-induced decrease in AMPAR-mEPSC frequency in CGCs is that NRG1 influences vesicle release probability. For example, activation of postsynaptic ErbB4 could affect presynaptic function by regulating the synthesis of retrograde signaling molecules such as nitric oxide, that is believed to enhance presynaptic vesicle release at mossy fiber-granule cell synapses (D'Angelo et al., 2005). Consistent with this idea, NRG1 may affect the function of nNOS in CGCs through a mechanism that involves activation of MAP kinase (Krainock and Murphy, 2001); however, NRG1 has not been shown to affect neurotransmitter release in CGCs. In summary, although our studies do not eliminate the possibility that NRG1 can modulate presynaptic function, taken together with previous studies our results strongly suggest NRG1 may regulate activity-dependent synaptic trafficking of AMPARs in CGCs.

4.5 Summary and Conclusions

Our results demonstrate that acute NRG1 may regulate glutamatergic plasticity in CGCs. Specifically, although acute NRG1 does not influence AMPAR or NMDAR-mediated responses in CGCs under baseline conditions, NRG1 treatment results in a decrease in AMPAR-mEPSC frequency following chemically-induced potentiation of AMPAR-mEPSC frequency. While these results are consistent with the effects of NRG-1/ErbB4-signaling on plasticity of glutamatergic CA3→CA1 synapses in the hippocampus (Chen et al., 2010; Iyengar and Mott, 2008; Kwon et al., 2005; Kwon et al., 2008; Pitcher et al., 2008), the cellular mechanisms that underlie the effects observed in our study are likely direct. That is, NRG-1 associated changes in glutamatergic function likely involve activation of ErbB4 in the granule cells from which we recorded; whereas, in hippocampal pyramidal neurons the effects of NRG-1 are likely indirect given the absence of ErbB4 detection in these cells (Neddens and Buonanno, 2010; Vullhorst et al., 2009) and the importance of GABAergic (Chen et al., 2010; Woo et al., 2007) and dopamine signaling to mediate the response (Kwon et al., 2008). We hypothesize that high-glycine and NRG1/ ErbB-4 affect activity-dependent trafficking of AMPARs in CGCs. The results of this study demonstrate that CGCs provide a useful system for further investigating the effects of acute NRG1/ErbB4-signaling on glutamatergic plasticity.

Acknowledgments

This study was supported through a Henry Luce III Endowment award for distinguished scholarship. We thank Zhanyan Fu and Stefano Vicini for guidance regarding neuronal cell culture, electrophysiological recording and data analysis.

Abbreviations

AMPA	α-amino-3-hydroxyl-5-methyl-4-isoxazole-propionate
CGCs	cerebellar granule cells
chemLTP	high-glycine/0Mg^{2+}-induced LTP
KA	kainate
LTP	long-term potentiation

mEPSC	miniature excitatory post-synaptic currents
NMDA	N-methyl-D-aspartic acid
NRG1	neuregulin-1
PSD-95	post synaptic density 95
PDZ	post synaptic density 95-Drosophila disc large tumor suppressor-zonula occludens-1

References

Adlkofer K, Lai C. Role of neuregulins in glial cell development. Glia. 2000; 29:104–11. [PubMed: 10625327]

Buonanno A, Fischbach GD. Neuregulin and ErbB receptor signaling pathways in the nervous system. Curr Opin Neurobiol. 2001; 11:287–96. [PubMed: 11399426]

Chen YJ, Zhang M, Yin DM, Wen L, Ting A, Wang P, Lu YS, Zhu XH, Li SJ, Wu CY, Wang XM, Lai C, Xiong WC, Mei L, Gao TM. ErbB4 in parvalbumin-positive interneurons is critical for neuregulin 1 regulation of long-term potentiation. Proc Natl Acad Sci U S A. 2010; 107:21818–23. [PubMed: 21106764]

Condorelli DF, Dell'Albani P, Aronica E, Genazzani AA, Casabona G, Corsaro M, Balazs R, Nicoletti F. Growth conditions differentially regulate the expression of alpha-amino-3-hydroxy-5-methylisoxazole-4-propionate (AMPA) receptor subunits in cultured neurons. J Neurochen. 1993; 61:2133–9.

Cull-Candy SG, Brickley SG, Misra C, Feldmeyer D, Momiyama A, Farrant M. NMDA receptor diversity in the cerebellum: identification of subunits contributing to functional receptors. Neuropharmacology. 1998; 37:1369–80. [PubMed: 9849672]

D'Angelo E, Rossi P, Armano S, Taglietti V. Evidence for NMDA and mGlu receptor-dependent long-term potentiation of mossy fiber-granule cell transmission in rat cerebellum. J Neurophysiol. 1999; 81:277–87. [PubMed: 9914288]

D'Angelo E, Rossi P, Gall D, Prestori F, Nieus T, Maffei A, Sola E. Long-term potentiation of synaptic transmission at the mossy fiber-granule cell relay of cerebellum. Prog Brain Res. 2005; 148:69–80. [PubMed: 15661182]

Farrant M, Feldmeyer D, Takahashi T, Cull-Candy SG. NMDA-receptor channel diversity in the developing cerebellum. Nature. 1994; 368:335–9. [PubMed: 7907398]

Fazzari P, Paternain AV, Valiente M, Pla R, Lujan R, Lloyd K, Lerma J, Marin O, Rico B. Control of cortical GABA circuitry development by Nrg1 and ErbB4 signalling. Nature. 2010; 464:1376–80. [PubMed: 20393464]

Fischbach GD, Rosen KM. ARIA: a neuromuscular junction neuregulin. Annu Rev Neurosci. 1997; 20:429–58. [PubMed: 9056721]

Fu Z, Logan SM, Vicini S. Deletion of the NR2A subunit prevents developmental changes of NMDA-mEPSCs in cultured mouse cerebellar granule neurones. J Physiol. 2005; 563:867–81. [PubMed: 15649973]

Gallo V, Upson LM, Hayes WP, Vyklicky L Jr, Winters CA, Buonanno A. Molecular cloning and development analysis of a new glutamate receptor subunit isoform in cerebellum. J Neurosci. 1992; 12:1010–23. [PubMed: 1372042]

Garcia RA, Vasudevan K, Buonanno A. The neuregulin receptor ErbB-4 interacts with PDZ-containing proteins at neuronal synapses. Proc Natl Acad Sci U S A. 2000; 97:3596–601. [PubMed: 10725395]

Huang YZ, Won S, Ali DW, Wang Q, Tanowitz M, Du QS, Pelkey KA, Yang DJ, Xiong WC, Salter MW, Mei L. Regulation of neuregulin signaling by PSD-95 interacting with ErbB4 at CNS synapses. Neuron. 2000; 26:443–55. [PubMed: 10839362]

Iyengar SS, Mott DD. Neuregulin blocks synaptic strengthening after epileptiform activity in the rat hippocampus. Brain Res. 2008; 1208:67–73. [PubMed: 18387600]

Krainock R, Murphy S. Regulation of functional nitric oxide synthase-1 expression in cerebellar granule neurons by heregulin is post-transcriptional, and involves mitogen-activated protein kinase. J Neurochem. 2001; 78:552–9. [PubMed: 11483658]

Kwon OB, Longart M, Vullhorst D, Hoffman DA, Buonanno A. Neuregulin-1 reverses long-term potentiation at CA1 hippocampal synapses. J Neurosci. 2005; 25:9378–83. [PubMed: 16221846]

Kwon OB, Paredes D, Gonzalez CM, Neddens J, Hernandez L, Vullhorst D, Buonanno A. Neuregulin-1 regulates LTP at CA1 hippocampal synapses through activation of dopamine D4 receptors. Proc Natl Acad Sci U S A. 2008; 105:15587–92. [PubMed: 18832154]

Liao D, Scannevin RH, Huganir R. Activation of silent synapses by rapid activity-dependent synaptic recruitment of AMPA receptors. J Neurosci. 2001; 21:6008–17. [PubMed: 11487624]

Longone P, Impagnatiello F, Mienville JM, Costa E, Guidotti A. Changes in AMPA receptor-spliced variant expression and shift in AMPA receptor spontaneous desensitization pharmacology during cerebellar granule cell maturation in vitro. J Mol Neurosci. 1998; 11:23–41. [PubMed: 9826784]

Losi G, Prybylowski K, Fu Z, Luo JH, Vicini S. Silent synapses in developing cerebellar granule neurons. J Neurophysiol. 2002; 87:1263–70. [PubMed: 11877500]

Lu C, Fu Z, Karavanov I, Yasuda RP, Wolfe BB, Buonanno A, Vicini S. NMDA receptor subtypes at autaptic synapses of cerebellar granule neurons. J Neurophysiol. 2006; 96:2282–94. [PubMed: 16885526]

Lu W, Man H, Ju W, Trimble WS, MacDonald JF, Wang YT. Activation of synaptic NMDA receptors induces membrane insertion of new AMPA receptors and LTP in cultured hippocampal neurons. Neuron. 2001; 29:243–54. [PubMed: 11182095]

Ma L, Huang YZ, Pitcher GM, Valtschanoff JG, Ma YH, Feng LY, Lu B, Xiong WC, Salter MW, Weinberg RJ, Mei L. Ligand-dependent recruitment of the ErbB4 signaling complex into neuronal lipid rafts. J Neurosci. 2003; 23:3164–75. [PubMed: 12716924]

Maffei A, Prestori F, Rossi P, Taglietti V, D'Angelo E. Presynaptic current changes at the mossy fiber-granule cell synapse of cerebellum during LTP. J Neurophysiol. 2002; 88:627–38. [PubMed: 12163516]

Mogensen HS, Jorgensen OS. AMPA receptor subunit mRNAs and intracellular [Ca(2+)] in cultured mouse and rat cerebellar granule cells. Int J Dev Neurosci. 2000; 18:61–8. [PubMed: 10708907]

Murase K, Ryu PD, Randic M. Tachykinins modulate multiple ionic conductances in voltage-clamped rat spinal dorsal horn neurons. Journal of neurophysiology. 1989; 61:854–65. [PubMed: 2470866]

Murphy SP, Bielby-Clarke K. Neuregulin signaling in neurons depends on ErbB4 interaction with PSD-95. Brain Res. 2008; 1207:32–5. [PubMed: 18374309]

Neddens J, Buonanno A. Selective populations of hippocampal interneurons express ErbB4 and their number and distribution is altered in ErbB4 knockout mice. Hippocampus. 2010; 20:724–44. [PubMed: 19655320]

Neddens J, Fish KN, Tricoire L, Vullhorst D, Shamir A, Chung W, Lewis DA, McBain CJ, Buonanno A. Conserved Interneuron-Specific ErbB4 Expression in Frontal Cortex of Rodents, Monkeys, and Humans: Implications for Schizophrenia. Biological Psychiatry. 2011

Ozaki M, Sasner M, Yano R, Lu HS, Buonanno A. Neuregulin-beta induces expression of an NMDA-receptor subunit. Nature. 1997; 390:691–4. [PubMed: 9414162]

Pickard L, Noel J, Duckworth JK, Fitzjohn SM, Henley JM, Collingridge GL, Molnar E. Transient synaptic activation of NMDA receptors leads to the insertion of native AMPA receptors at hippocampal neuronal plasma membranes. Neuropharmacology. 2001; 41:700–13. [PubMed: 11640924]

Pitcher GM, Beggs S, Woo RS, Mei L, Salter MW. ErbB4 is a suppressor of long-term potentiation in the adult hippocampus. Neuroreport. 2008; 19:139–43. [PubMed: 18185097]

Prybylowski K, Fu Z, Losi G, Hawkins LM, Luo J, Chang K, Wenthold RJ, Vicini S. Relationship between availability of NMDA receptor subunits and their expression at the synapse. J Neurosci. 2002; 22:8902–10. [PubMed: 12388597]

Rieff HI, Raetzman LT, Sapp DW, Yeh HH, Siegel RE, Corfas G. Neuregulin induces GABA(A) receptor subunit expression and neurite outgrowth in cerebellar granule cells. J Neurosci. 1999; 19:10757–66. [PubMed: 10594059]

Rieff HI, Corfas G. ErbB receptor signalling regulates dendrite formation in mouse cerebellar granule cells in vivo. Eur J Neurosci. 2006; 23:2225–9. [PubMed: 16630068]

Rio C, Rieff HI, Qi P, Khurana TS, Corfas G. Neuregulin and erbB receptors play a critical role in neuronal migration. Neuron. 1997; 19:39–50. [PubMed: 9247262]

Shepherd JD, Huganir RL. The cell biology of synaptic plasticity: AMPA receptor trafficking. Annu Rev Cell Dev Biol. 2007; 23:613–43. [PubMed: 17506699]

Shi SH, Hayashi Y, Petralia RS, Zaman SH, Wenthold RJ, Svoboda K, Malinow R. Rapid spine delivery and redistribution of AMPA receptors after synaptic NMDA receptor activation. Science. 1999; 284:1811–6. [PubMed: 10364548]

Siegelbaum SA, Kandel ER. Learning-related synaptic plasticity: LTP and LTD. Current opinion in neurobiology. 1991; 1:113–20. [PubMed: 1822291]

Silver RA, Traynelis SF, Cull-Candy SG. Rapid-time-course miniature and evoked excitatory currents at cerebellar synapses in situ. Nature. 1992; 355:163–6. [PubMed: 1370344]

Ting AK, Chen Y, Wen L, Yin DM, Shen C, Tao Y, Liu X, Xiong WC, Mei L. Neuregulin 1 promotes excitatory synapse development and function in GABAergic interneurons. J Neurosci. 2011; 31:15–25. [PubMed: 21209185]

Turecek R, Vlachova V, Vyklicky L Jr. Spontaneous openings of NMDA receptor channels in cultured rat hippocampal neurons. The European Journal of Neuroscience. 1997; 9:1999–2008. [PubMed: 9421161]

Vullhorst D, Neddens J, Karavanova I, Tricoire L, Petralia RS, McBain CJ, Buonanno A. Selective expression of ErbB4 in interneurons, but not pyramidal cells, of the rodent hippocampus. J Neurosci. 2009; 29:12255–64. [PubMed: 19793984]

Woo RS, Li XM, Tao Y, Carpenter-Hyland E, Huang YZ, Weber J, Neiswender H, Dong XP, Wu J, Gassmann M, Lai C, Xiong WC, Gao TM, Mei L. Neuregulin-1 enhances depolarization-induced GABA release. Neuron. 2007; 54:599–610. [PubMed: 17521572]

Xie F, Raetzman LT, Siegel RE. Neuregulin induces GABAA receptor beta2 subunit expression in cultured rat cerebellar granule neurons by activating multiple signaling pathways. J Neurochem. 2004; 90:1521–9. [PubMed: 15341535]

Xie F, Padival M, Siegel RE. Association of PSD-95 with ErbB4 facilitates neuregulin signaling in cerebellar granule neurons in culture. J Neurochem. 2007; 100:62–72. [PubMed: 17074065]

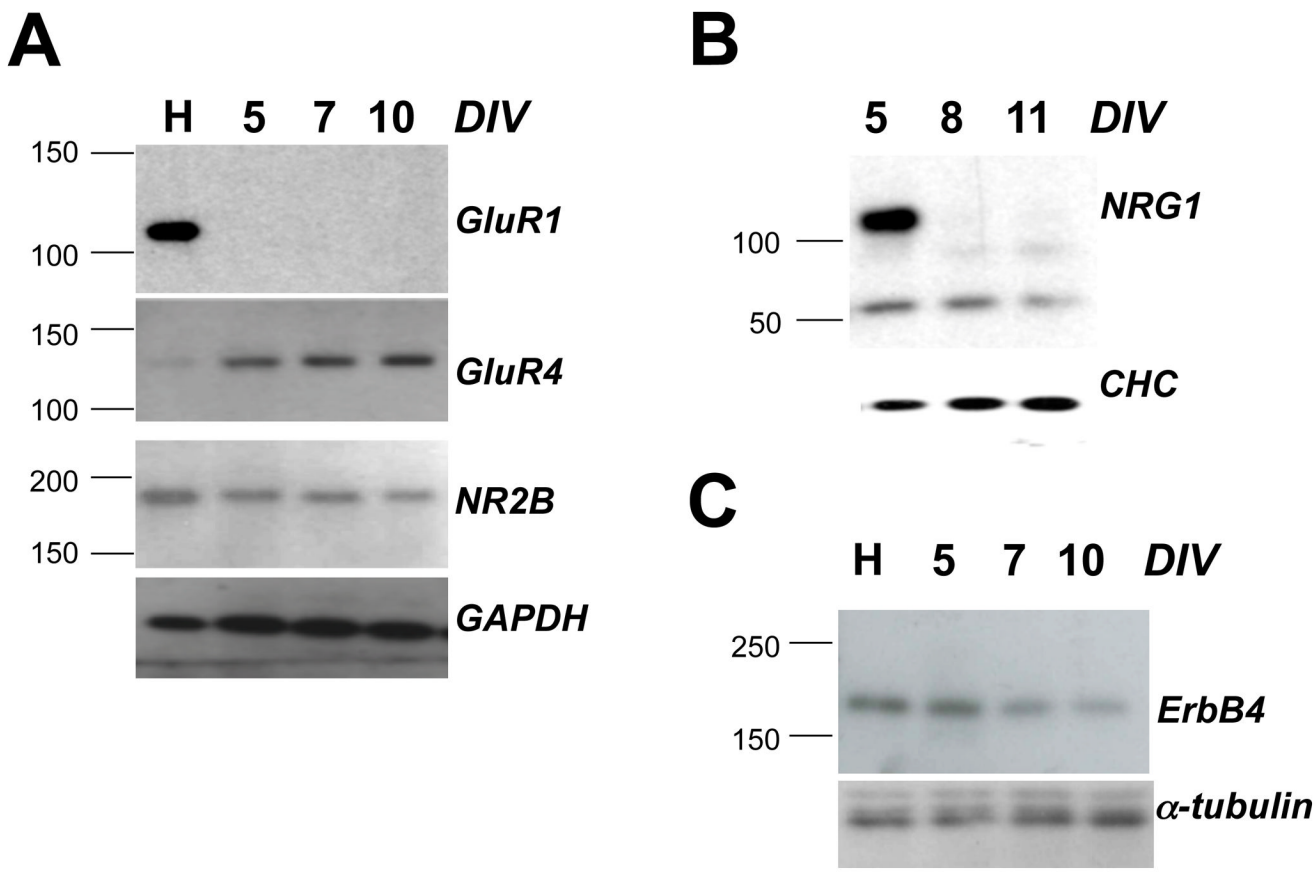

Fig. 1. Expression of GluR1, GluR4 long, NR2B, ErbB4 and NRG1 in CGCs

Protein extracts from DIV 5–11 CGCs and DIV 16 hippocampal neurons (20 μg per lane) were tested for expression of GluR1, GluR4 long, and NR2B (A), ErbB4 (B), and NRG1 (C). Primary antibodies for indicated proteins are described in Materials and Methods. Hippocampal lysates (**H**) from primary cultures at DIV 16 were included as reference. Days *in vitro* (*DIV*) for CGCs are indicated above the lanes. GAPDH, α-tubulin and clathrin heavy chain (CHC) immunoreactivities served as loading controls.

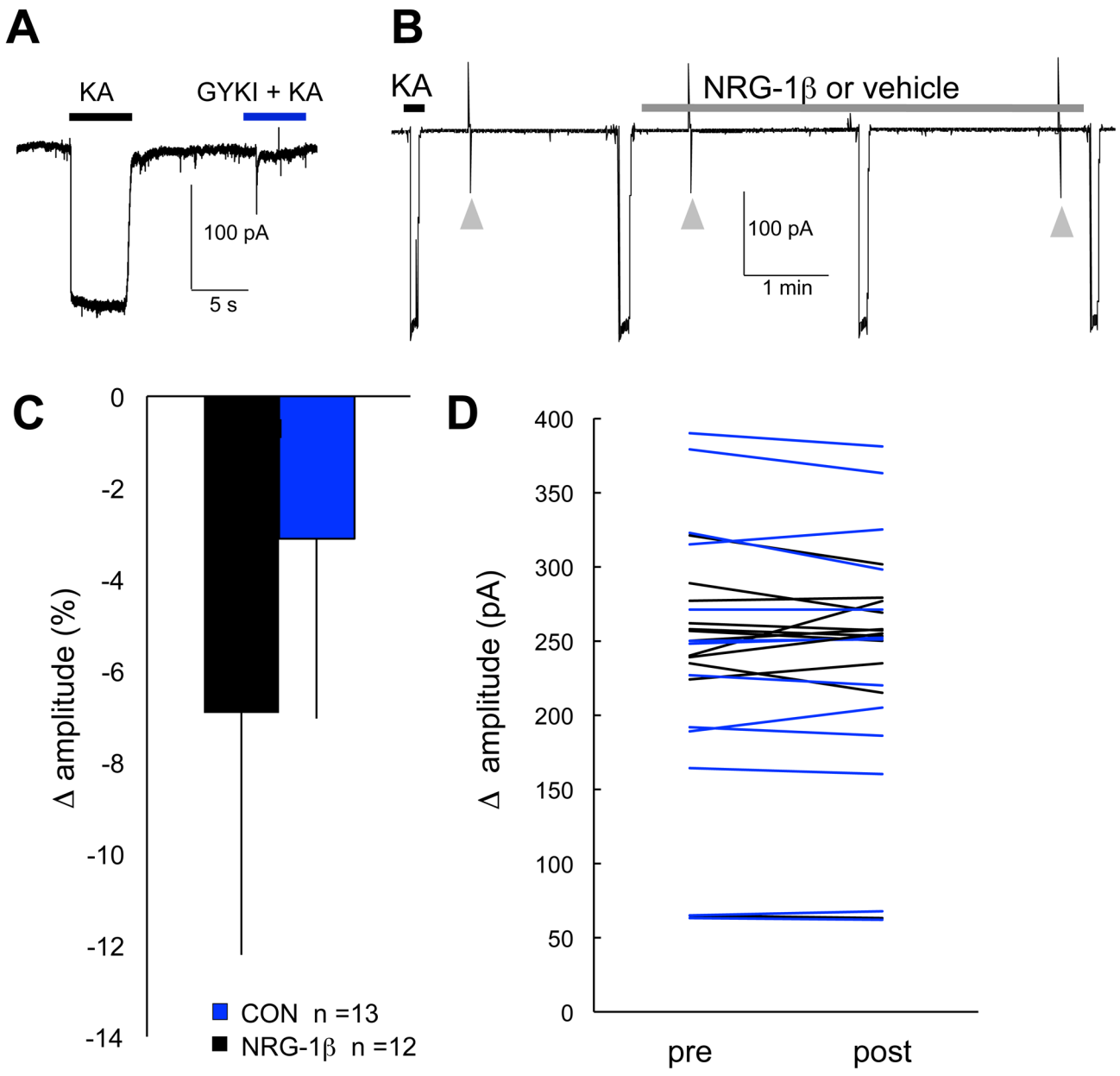

Fig. 2. NRG1 does not affect whole-cell AMPAR-mediated currents under baseline conditions

(A) Representative trace showing whole-cell AMPAR currents in response to 50 μM kainate (KA), which primarily activates AMPAR, as demonstrated by blockade with 50 μM GYKI-52466 (GYKI). (B) Experimental protocol used to assess whole-cell KA responses prior to and during NRG1 or vehicle control in CGCs at 9–12 DIV. Arrowheads indicate transient currents in response to 5 mV step pulses used to monitor access resistance. TTX, bicuculline and Mg^{2+} were present in the recording and bath perfusion solutions. (C) Bars plot mean (±SD) for change in peak whole-cell KA current amplitudes (calculated as the average of two peak amplitudes post-treatment minus baseline). (D) Lines show KA current amplitudes for individual cells prior to and following treatment with NRG1 (black lines) or control (blue lines).

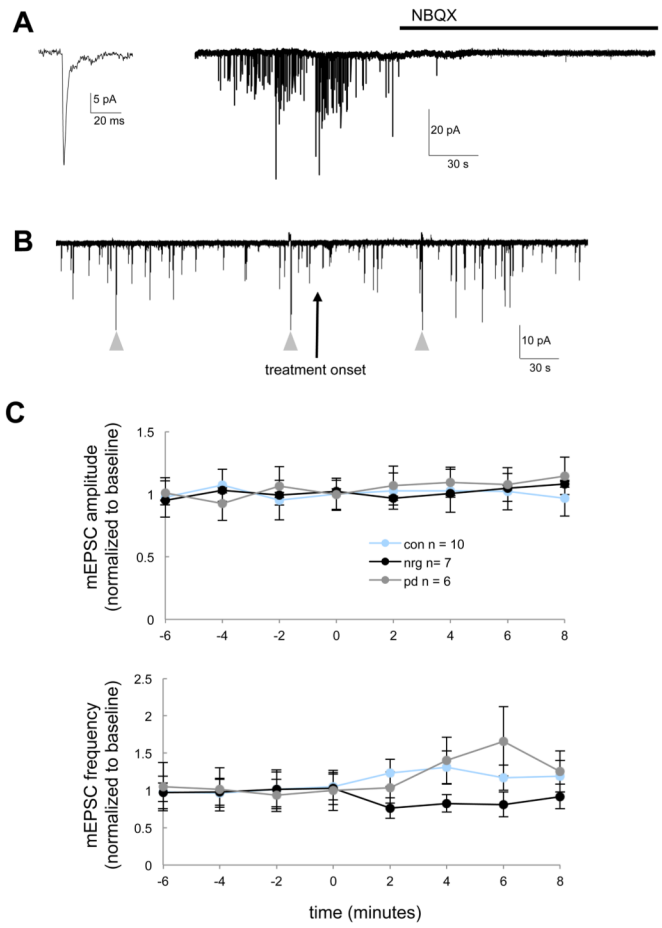

Fig. 3. AMPAR-mediated mEPSCs are not affected by NRG1 or PD158780 under baseline conditions for CGCs

(A) AMPAR-mEPSCs were recorded from CGCs at 10–12 DIV in the presence of TTX, bicuculline and 1 mM Mg^{2+} at a holding potential of −60 mV. AMPAR-mEPSCs were blocked by NBQX as indicated (10 μM). (B) Experimental protocol used to assess AMPA-mEPSCs prior to and following treatment with either NRG1 (2nM), the pan ErbB kinase inhibitor PD158780 (10 μM) or vehicle. Arrowheads indicate transient currents in response to 5 mV steps used to monitor access resistance. (C) AMPAR-mEPSC amplitude and frequency were not affected by either NRG1 or ErbB-blockade. Data points represent mean (±SEM) amplitude and frequency (normalized to baseline) for AMPAR-mEPSC occurring during 30–60 sec of continuous recording at indicated time points prior to following treatment onset.

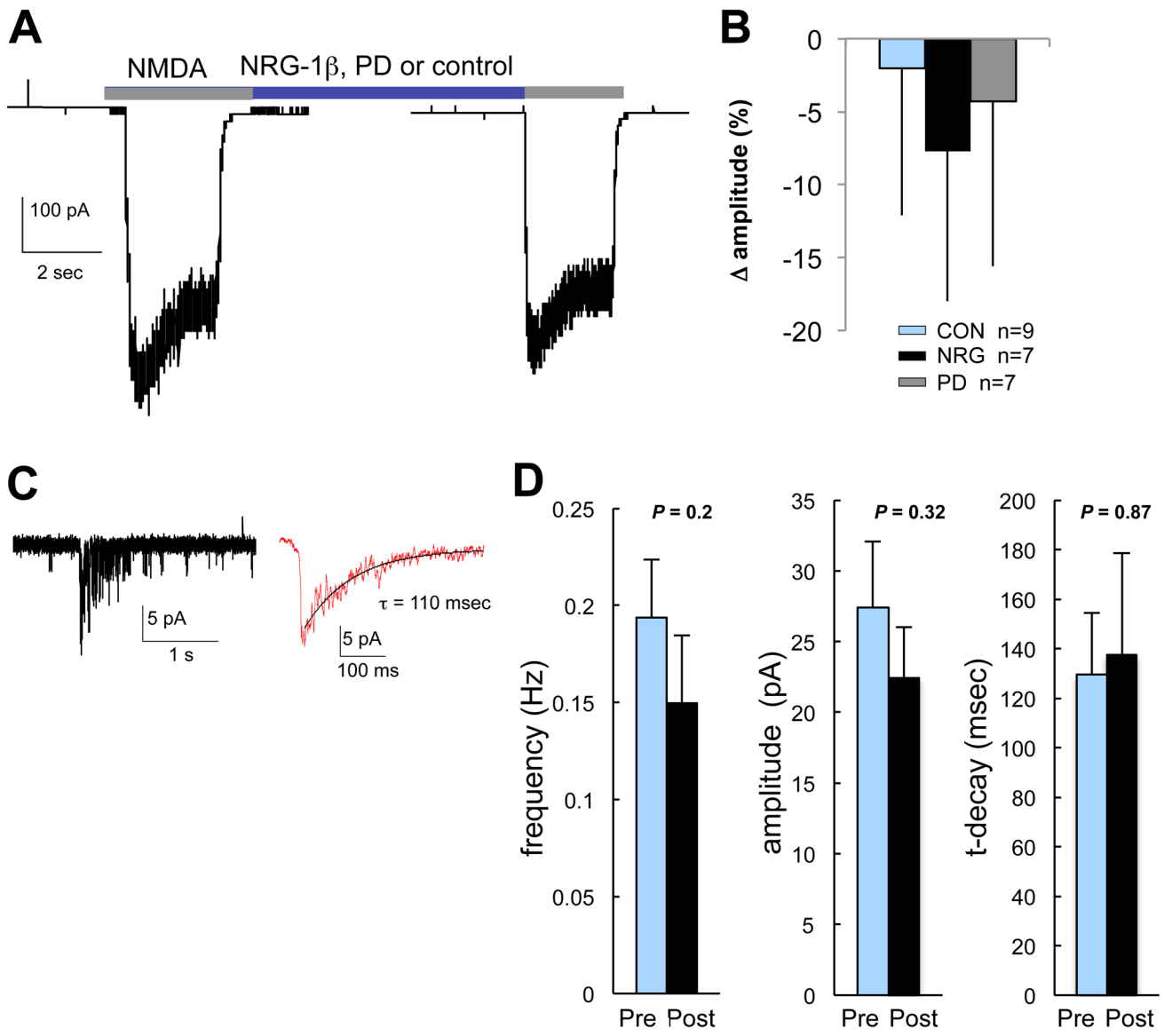

Fig. 4. Acute NRG1 treatment does not affect the function of NMDAR in CGCs

(A) Experimental design for assessing effects of NRG1/ErbB-signaling on whole-cell NMDAR currents for CGCs (10–12 DIV). Whole-cell NMDAR currents in response to 200 μM NMDA were measured before and after 2–4 min exposure to NRG1, PD158780 or vehicle control. (B) Bars plot mean (and SD) change in whole-cell current amplitude (calculated as % of the amplitude prior to treatment onset). No differences in the change in current amplitude were observed between treatment groups ($F_{(2,22)} = 0.63$, $P = 0.54$; one-way ANOVA). (C) NMDAR-mEPSCs were isolated by recording at −60 mV in ECF containing 0 Mg^{2+}, 5 μM NBQX, 50 μM bicuculline. The figure shows a single and averaged NMDAR-mEPSC (average of 10–20 consecutive events) from which decay time constants (τ) were fit using a single exponential function. (D) Bars plot mean (and SEM) peak current amplitude, frequency and τ-decay following treatment with NRG1 or vehicle (*P*-values for paired Student's t-tests are indicated, n= 7). Mean frequency, amplitude and τ-decay for NMDA-mEPSCs were analyzed from events occurring during one minute of

continuous recording within the 2 min prior to treatment and within 2–4 min following treatment onset.

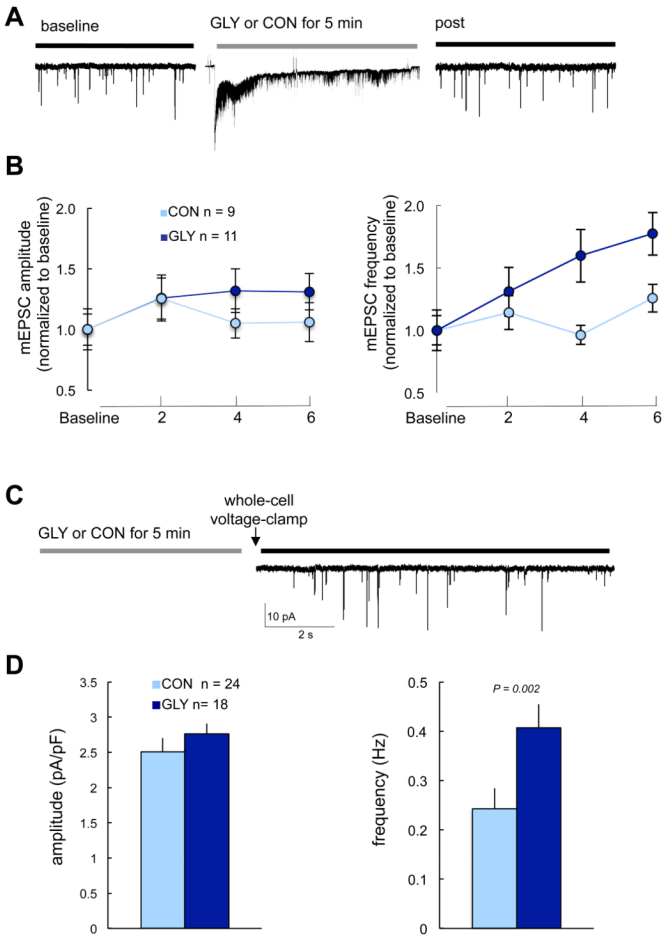

Fig. 5. High-glycine/0 Mg^{2+} potentiates AMPA-mEPSC frequency, but not amplitude, for CGCs

(A) Experimental protocol used to assess effects of high-glycine/0Mg^{2+} on AMPA-mEPSC frequency and amplitude. Cells were voltage-clamped continuously prior to, during and following glycine treatment (200 μM glycine (GLY) in Mg^{2+}-free ECF containing bicuculline and strychnine, RT for 5 min). (B) Results of experiments outlined in A, showing high-glycine is associated with increased AMPAR-mEPSC frequency, but not amplitude. Data points plot mean (± SEM) normalized to baseline pretreatment values for comparison purposes. Amplitudes represent averages of AMPAR-mEPSCs occurring during 30–60 sec continuous recording at indicated time points. The change in frequency was greater for glycine treated cells. $^{**}P = 0.02$. (C) Experimental protocol used to assess the effects of high-glycine/0 Mg^{2+} on AMPAR-mEPSCs in which cells were treated with high-glycine/0 Mg^{2+} immediately prior to going whole-cell. (D) Results of experimental protocol outlined in C. Bars plot mean (and SEM) frequency and amplitude for AMPAR-mEPSCs occurring during 60 sec continuous recording within 4–6 min of voltage-clamping and within 6–8 min of glycine treatment. *P*-values indicate results of independent sample *t*-tests.

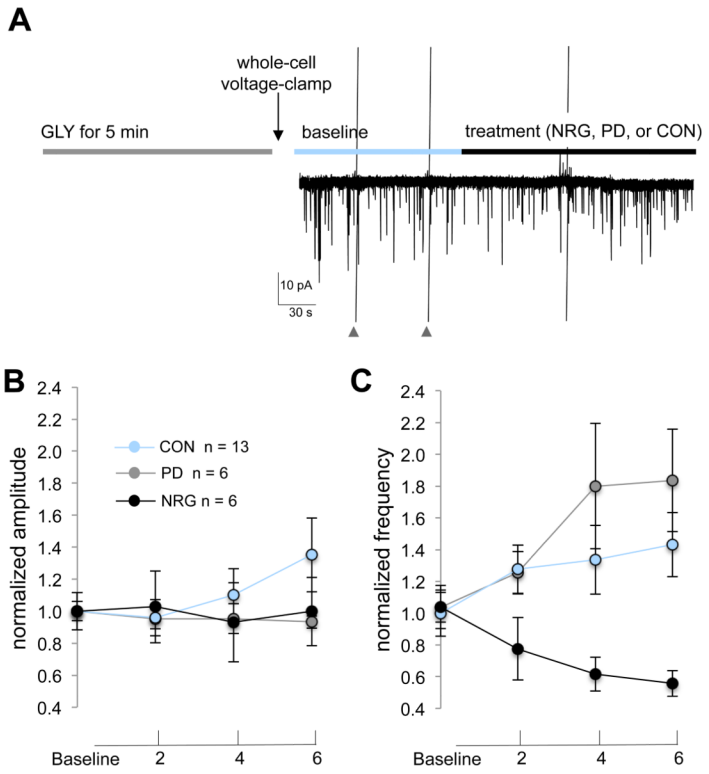

Fig. 6. NRG1 reduces AMPAR-mEPSC frequency, but not amplitude, following chemLTP

(A) Experimental protocol used to assess effects of treatments following high-glycine. Cells were immediately voltage-clamped following exposure to high-glycine and baseline data were collected for 4–6 min prior to and following treatment onset with either PD158780, NRG1, or vehicle control. Data points plot mean (± SEM) AMPA-mEPSC amplitude (B) and frequency (C) at baseline and at indicated time points following treatments. Data points were normalized for comparison purposes. Baseline values reflect the average amplitude and frequency of AMPA-mEPSCs during 60 sec of continuous recording (at 3 min and 0 min prior to treatment onset) and at indicated time points following treatment onset. ** $P<0.001$ (repeated measures ANOVA, time*treatment interaction).